Acta Crystallographica Section A
Foundations of Crystallography
ISSN 0108-7673

Received 17 November 2008
Accepted 25 May 2009

Towards the best model for H atoms in experimental charge-density refinement

Anna A. Hoser, Paulina M. Dominiak and Krzysztof Woźniak*

Chemistry Department, Warsaw University, 02-093 Warszawa, Pasteura 1, Poland.
Correspondence e-mail: kwozniak@chem.uw.edu.pl

The consequences of different treatments of H atoms in experimental charge-density studies are discussed. Geometric and topological parameters obtained after applying four different H-atom models in multipolar refinement on high-resolution X-ray data only were compared with the results obtained for a reference joint high-resolution X-ray/neutron refinement. The geometry and the topological critical point and integrated parameters closest to the reference values were obtained after a mixed refinement (high-order refinement of heavy atoms, low-angle refinement of H atoms and elongation of the X—H distance to the average neutron bond lengths) supplemented by an estimation of the anisotropic thermal motions of H atoms using the *SHADE* program. Such a procedure works very well even for strong hydrogen bonds. The worst fit to the reference results for both critical point and integrated parameters was obtained when only the standardization to the average neutron X—H distances was applied. The non-H-atom parameters are also systematically influenced by the H-atom modeling. In order to compare topological and integrated properties calculated for H and non-H atoms in multipolar refinement when there are no neutron data, the same treatment of H atoms (ideally the mixed refinement + estimated anisotropic atomic displacement parameters for H atoms) should be applied.

1. Introduction

Establishing a three-dimensional crystal structure for a small organic or inorganic compound is not sufficient in the context of studies of inter- and intramolecular interactions. Much more information about chemical bonding and one-electron properties in the crystalline state can be obtained after performing refinement of charge density against high-resolution X-ray diffraction data. Experimental charge-density studies have been developing intensively over the past two decades and they are now an important source of information in many branches of chemistry and materials studies (Koritsanszky & Coppens, 2001). The multipole refinement of good quality experimental data can give detailed information on charge-density distribution over a molecule and makes possible the analysis of fine electron effects in the solid state, which is still very difficult using *ab initio* approaches.

To obtain reliable information about the charge-density distribution, the X-ray diffraction data must be collected to the highest possible resolution so that atomic positions and thermal motions can be defined accurately. The accuracy and precision of the final experimental electron-density distribution also depend strongly on the quality of work of a given experimentalist, on the quality of models applied to describe the electron density and on approximations made to deconvolute thermal motion from the static electron density. In particular, the positions and thermal motions of H atoms are of paramount importance to estimate reliably the properties derived from the crystal electron density (see *e.g.* Stewart, 1991; Spackman, 1992, 1999; Chen & Craven, 1995; Spackman & Byrom, 1996; Espinosa *et al.*, 1998; Roversi & Destro, 2004; Espinosa, Lecomte & Molins, 1999; Espinosa, Souhassou *et al.*, 1999; Spackman *et al.*, 1999).

The positions and atomic displacement parameters of H atoms can be determined far more precisely and accurately from neutron diffraction. It is therefore recommended to supplement high-resolution X-ray data refinement with nucleic parameters of H atoms taken from a neutron diffraction experiment. However, neutron methods have serious limitations, such as the availability of neutron sources and the size of crystals required for neutron studies. As a result, only a few joint high-resolution X-ray/neutron multipolar refinements are published per year [*ca* 30 from 1999 to 2007; see Fig. 1 of Munshi *et al.* (2008)].

The vast majority of experimental charge-density investigations are based on different types of approximations to the neutron data. In particular, diverse methods to describe H-atom positions and thermal motion are applied. Because the refinement of X-ray data shortens the X—H bond lengths, the most common practice used is that the H-atom positions are shifted, maintaining the direction of bonds, in such a way as to obtain average neutron bond lengths characteristic of a

given type of X—H bond. In the case of thermal motions of H atoms most researchers apply the simplest isotropic displacement model.

The next most commonly used model for H atoms employs a high-order refinement. In principle, the high-order (usually $\sin\theta/\lambda \geq 0.7$ Å^{-1}) refinement leads to precise positional and displacement parameters of atoms comparable to those obtained from neutron diffraction. However, the low scattering power of hydrogen at a high scattering angle often prevents the inclusion of H-atom parameters in the high-order refinement. In such a case, high-order refinement for non-H atoms and low-order refinement together with X—H bond standardization for H atoms is performed (see *e.g.* Wolstenholme *et al.*, 2006; Kocher *et al.*, 2004). For the purpose of this paper we will call such a refinement a 'mixed' one. In both versions of the high-order refinement, an isotropic model of atomic displacements of H atoms is applied.

Another approach to H-atom modeling is based on an estimation of anisotropic atomic displacement parameters (ADPs). The first publications in which H-atom thermal motion was described by estimated ADPs appeared in 1975 (Harel & Hirshfeld, 1975; Hirshfeld, 1976; Hirshfeld & Hope, 1980; Eisenstein & Hirshfeld, 1983). Since then a lot has been done in the field (Destro & Merati, 1995; Chen & Craven, 1995; Roversi *et al.*, 1996; Flaig *et al.*, 1998; Roversi & Destro, 2004). It appears that ADPs of H atoms can be estimated quite well and are close to those obtained from neutron diffraction experiments (Munshi *et al.*, 2008). This approach is especially good for small and rigid molecules.

It has recently been shown that a proper description of thermal motion is crucial in charge-density studies (Koritsanszky & Coppens, 2001; Madsen *et al.*, 2004; Spackman *et al.*, 2007). The benefits of the use of anisotropic over isotropic displacement parameters for H atoms in charge-density studies were set out by Madsen *et al.* (2004). For the best isotropic and best anisotropic models of H atoms, the values of charge density, ρ(BCP), and Laplacian, $\nabla^2\rho$(BCP), at critical points (BCPs) of covalent bonds were compared with the values obtained from a reference model. In the reference model, H-atom positions and ADPs were taken from neutron diffraction measurements. It appears that applying the isotropic model of H atoms 'is highly unsatisfactory and leads to significant deviations for the properties of the bond critical points including those that only involve non-H atoms' (Madsen *et al.*, 2004). It is surprising then that isotropic displacement parameters for H atoms are still commonly used in about 80% of reported charge-density studies (Munshi *et al.*, 2008).

In this work we investigate the importance of positions and ADPs of H atoms for characterizing weak interactions, hydrogen bonding in particular. We extended the analysis beyond the point properties of BCPs and included integrated atomic properties of H atoms involved in hydrogen bonding. These parameters were not analyzed in this context earlier. Reliable values of topological properties such as ρ(BCP), $\nabla^2\rho$(BCP), integrated atomic charge, integrated atomic volume and magnitude of integrated atomic dipole moment are crucial to verify the existence of weak interactions according to the Koch & Popelier (1995) criteria.

As model compounds we chose a series of 1,8-bis-(dimethylamino)naphthalene (DMAN) salts of organic counter-ions: 4,5-dichlorophthalic acid (DMANH$^+$dCldCA$^-$), *o*-benzoic sulfimide dihydrate (saccharin; DMANH$^+$SAC$^-$) and 1,2,4,5-benzenetetracarboxylic acid (pyromellitic acid; DMANH$^+$tCA$^-$) (see Fig. 1). These compounds have been extensively studied in our laboratory (Dominiak *et al.*, 2006; Woźniak *et al.*, 2003; Mallinson *et al.*, 2003). DMAN is a parent molecule of a class of compounds known as proton sponges (Staab & Saupe, 1988). They can easily drag hydrogen from counter-moieties and, in consequence, form ionic salts containing the DMANH$^+$ cation. In this cation, there is quite a strong [N···H···N]$^+$ hydrogen bond. Usually, it is slightly asymmetric, supported by charge conjugated with the π-electron density of the aromatic rings. In two of the anions (see Figs. 1*b* and 1*d*), very strong, almost symmetric [O···H···O]$^-$ hydrogen bonds are formed. Additionally, a number of weak C—H···O hydrogen bonds exist between the cation and O atoms of the anions (Fig. 2).

It appears that, in the case of DMAN salts, application of the common procedure of extending the X—H bond lengths to the standardized neutron values (selected by Madsen and co-workers to be the best positional model) leads to H-atom positions far from those obtained when real neutron data are used. Therefore, in the present work we search for a better model of positional parameters of H atoms. Knowing that, to describe properly H-atom motion, anisotropic ADPs are needed, we also explore whether ADPs estimated for H atoms involved in strong hydrogen bonding are good enough to benefit charge-density studies through their use. In addition, we check whether or not the truncation level of multipolar expansion on H atoms (up to dipoles or quadrupoles) influences the performance of selected positional and atomic motion models of H atoms. Finally, we consider the magnitude of the effects of different methods of H-atom treatment on the point and integrated topological properties.

2. Experimental

Several types of charge-density refinements were performed for three DMAN complexes (Fig. 1). Measurement details of neutron and X-ray diffraction data are described by Mallinson *et al.* (2003). All structures were solved and refined using an

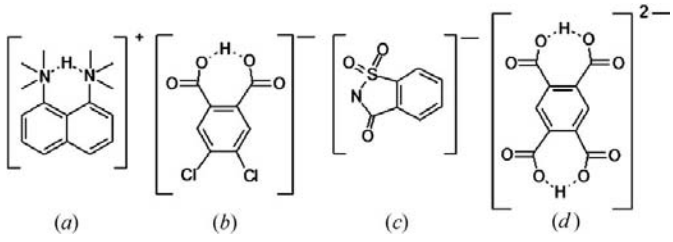

Figure 1
Schemes of (*a*) the DMANH$^+$ cation and organic anions from the (*b*) DMANH$^+$dCldCA$^-$, (*c*) DMANH$^+$SAC$^-$ and (*d*) DMANH$^+$tCA$^-$ salts.

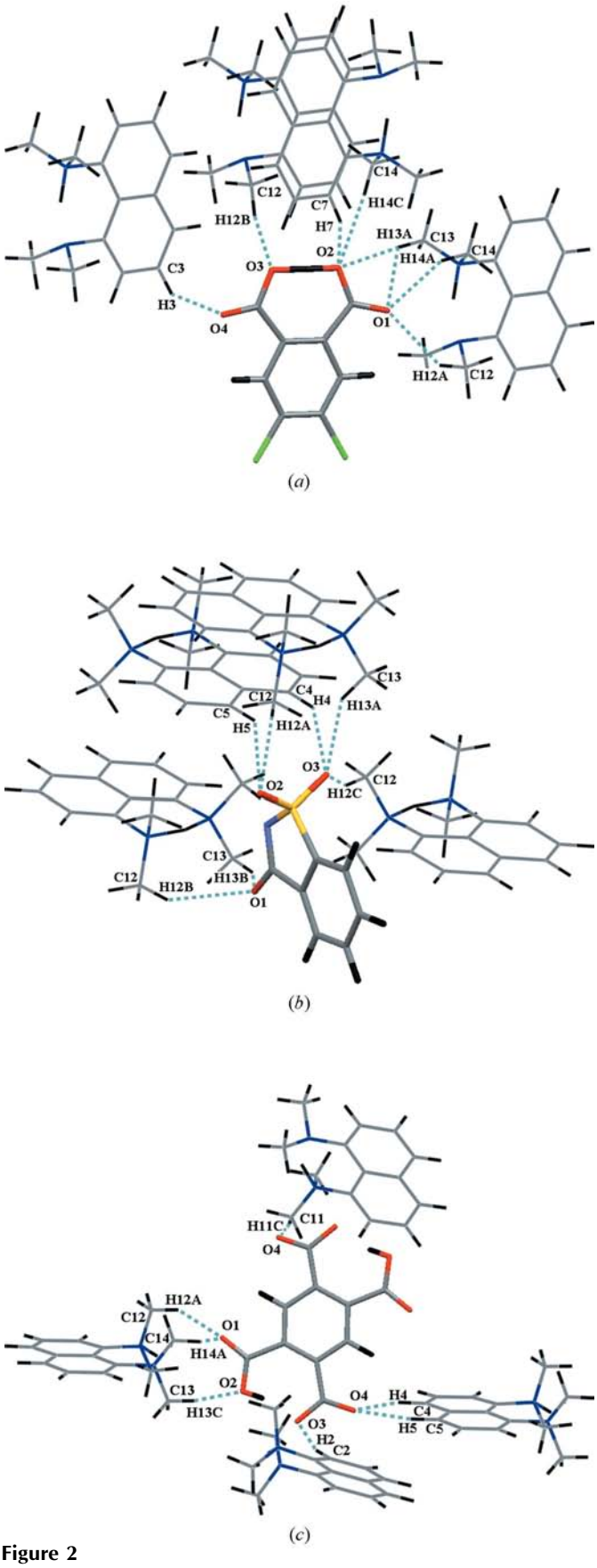

Figure 2
C—H···O intermolecular interactions in (*a*) $DMANH^{+}dCldCA^{-}$, (*b*) $DMANH^{+}SAC^{-}$ and (*c*) $DMANH^{+}tCA^{-}$.

independent atom model (IAM) in *SHELX* (Sheldrick, 2008). Subsequently, multipolar refinement on F^2 was performed in *XD* (Koritsanszky *et al.*, 1997). The set of refined parameters was gradually increased in the following order: (1) scale factor; (2) positions and ADPs for non-H atoms;[1] (3) valence populations and (4) dipoles for all atoms; (5) quadrupoles for non-H atoms only (refinements marked as _D) or for all atoms (refinements marked as _Q); (6) octupoles for non-H atoms; (7) hexadecapoles for Cl and S atoms; (8) contraction/expansion coefficients κ and κ' for non-H atoms. κ and κ' for C atoms were divided into three groups: aromatic, methyl and acidic. Usually κ and κ' for non-H atoms were refined, but whenever refinement did not converge or κ' had a nonphysical value, they were fixed on theoretical values[2] (Volkov *et al.*, 2001). For H atoms, κ and κ' were always fixed at theoretical values (1.13 and 1.29, respectively; Volkov *et al.*, 2001).

For each DMAN complex, six different treatments of H-atom positions and displacement parameters were tested (Table 1):

(1) NEUT – positions and ADPs were taken from neutron diffraction data. No scaling of neutron ADPs to X-ray data was needed. Positions and ADPs for H atoms were fixed in the course of multipolar refinement, whereas for non-H atoms they were further refined.

(2) MI_RB – for non-H atoms, high-order refinement of positions and ADPs was performed ($\sin\theta/\lambda > 0.6$ Å^{-1}), and then these parameters were fixed and refined only at the end of the multipolar refinement. Subsequently, low-order ($\sin\theta/\lambda < 0.6$ Å^{-1}) refinement was performed to find the best positions and isotropic displacement parameters for H atoms. After that, H atoms were shifted to the standard neutron X—H distances (1.08 Å for aromatic H atoms and 1.06 Å for methyl H atoms; Allen *et al.*, 1987) and their positions fixed. After refinement of the electron populations $P_{\rm val}$ and P_{lm}, and the κ and κ' parameters, the positions and ADPs for the non-H atoms were included in the refinement.

(3) RB – positions and isotropic displacement parameters for H atoms were taken from the IAM refinement. H atoms were then shifted to standard neutron X—H distances (Allen *et al.*, 1987) and their positions fixed.

(4) RB_SH – after IAM refinement the complexes were divided into individual moieties, and for each molecule ADPs for H atoms were generated by the *SHADE* program (*Simple Hydrogen Anisotropic Displacement Estimator*; Madsen, 2006). H atoms were then shifted to the standard neutron X—H distances (Allen *et al.*, 1987) and their positions fixed.

(5) MI_RB_SH – this method is a combination of the MI_RB and RB_SH methods. First, the positions and ADPs for all atoms were found from high/low-order refinement, then the H atoms were shifted to standard neutron X—H distances, and subsequently ADPs for H atoms were estimated by the

[1] In some refinement types (MI and MI_SH) the position and anisotropic ADPs for non-H atoms were treated in a special way as described below.
[2] This was done for $DMANH^{+}tCA^{-}$ in NEUT_D (κ' for N), NEUT_Q (κ' for C); $DMANH^{+}dCldCA^{-}$ in MI_RB_Q (κ' for N and C), RB_SH_Q (κ' for O, N, C); $DMANH^{+}SAC^{-}$ (in almost every refinement, κ' for O connected to S was fixed; also, for NEUT_D, NEUT_Q and RB_SH_Q, κ' for N, C was fixed).

Table 1
Definition of the refinement models.

R – parameters refined; F – parameters fixed; NF – parameters fixed on standard neutron diffraction distances; E – parameters estimated.

	C, O, N, S, Cl atoms			H atoms				
Model	*xyz*	U_{aniso}	Multipoles	*xyz*	U_{aniso}	U_{iso}	Dipoles	Quadrupoles
NEUT_D	R	R	R	F	F	–	R	–
NEUT_Q	R	R	R	F	F	–	R	R
MI_RB_D	R, F, R	R, F, R	R	R, NF	–	R, F	R	–
MI_RB_Q	R, F, R	R, F, R	R	R, NF	–	R, F	R	R
RB_D	R	R	R	NF (IAM)	–	F (IAM)	R	–
RB_Q	R	R	R	NF (IAM)	–	F (IAM)	R	R
RB_SH_D	R	R	R	NF (IAM)	E	–	R	–
RB_SH_Q	R	R	R	NF (IAM)	E	–	R	R
MI_RB_SH_D	R, F, R	R, F, R	R	R, NF	E	–	R	–
MI_RB_SH_Q	R, F, R	R, F, R	R	R, NF	E	–	R	R

SHADE program. After refinement of P_{val}, P_{lm}, κ and κ', the positions and ADPs for the non-H atoms were included in the refinement.

In each case H atoms involved in strong hydrogen bonds [$(N\cdots H\cdots N)^+$ and $(O\cdots H\cdots O)^-$] were not shifted to the standard neutron X—H distances, but their positions were taken directly either from IAM (RB, RB_SH) or mixed refinements (MI_RB, MI_RB_SH).

After each refinement atomic basin integration was performed in *TOPXD* in *XD2006* (Volkov *et al.*, 2000). The values of the integrated Lagrangian were less than 10^{-4} and 10^{-3} atomic units (a.u.) for hydrogen and the remaining atoms, respectively. Integrated atomic charges of asymmetric units summed to very small values (0.06*e* or less) and the sum of the atomic volumes reproduced the unit-cell volume per molecule with an error of 0.2% or less.

3. Results and discussion

3.1. Quality of refinements

Statistics characterizing the final refinements for the three compounds studied are listed in Table 2. All parameters, *i.e.* $R(F^2)$, $wR(F^2)$, goodness of fit (GOF) and residual densities, are comparable for different types of treatment of H-atom positions and displacement parameters. Small but systematic lowering of the parameters is observed for the refinements with quadrupoles on H atoms as opposed to dipoles. This could be associated with the increased number of refined parameters.

As clearly seen, the presented statistics are not good enough to establish the correctness of the multipolar model. Therefore for one selected compound, $DMANH^+dCldCA^-$, we applied a statistical significance test (Prince & Spiegelman, 1995) in order to find which of the compared models represents a better fit to the experimental data. For each pair of refinements two parameters, z and x, were calculated:

$$z = \left[F_o^2 - 0.5(F_{C1}^2 + F_{C2}^2)\right]/\sigma(F_o^2),$$
$$x = (F_{C1}^2 - F_{C2}^2)/\sigma(F_o^2), \quad (1)$$

where $C1$ and $C2$ denote the two different models used in the refinement. Then the slope (λ) and its estimated standard deviation (σ) for the regression line $z = \lambda x$ were found. When the first calculated model ($C1$) better fits the measured data, then the parameter λ is $ca +\frac{1}{2}$. When the second model ($C2$) is closer to the data, λ is $ca -\frac{1}{2}$. To verify the significance of λ, the statistic $t = |\lambda/\sigma|$ was calculated and tested by using the Student's t-test at the significance level $\alpha = 0.05\%$.

The results obtained are listed in Table 3. It appears that the differences for all pairs of compared models, except the differences between MI_RB_SH_Q and NEUT_Q, are statistically significant at $\alpha = 0.05\%$. When the same refinement protocols but with different truncation levels (dipoles or quadrupoles) on H atoms are compared, a better fit to the measured data is obtained when quadrupoles on H atoms are used. Since the differences are statistically significant, one may assume that the improvement of the fit represents additional information contained in the 'quadrupolar' model not taken into account by the model truncated at the dipole level. From comparison of the most advanced MI_RB_SH model with any other simpler one (RB, MI_RB and RB_SH), it is clear that it always gives a better fit to the measured data. Moreover, the MI_RB_SH_D model describes the experimental data significantly better than the reference NEUT_D does. In the case of MI_RB_SH_Q and NEUT_Q, both models are equally good.

Table 2
Refinement statistics for $DMANH^+dCldCA^-$, $DMANH^+SAC^-$ and $DMANH^+tCA^-$.

	$DMANH^+dCldCA^-$				$DMANH^+SAC^-$				$DMANH^+tCA^-$			
Model	$R(F^2)$	$wR(F^2)$	GOF	Residual density (e Å^{-3})	$R(F^2)$	$wR(F^2)$	GOF	Residual density (e Å^{-3})	$R(F^2)$	$wR(F^2)$	GOF	Residual density (e Å^{-3})
NEUT_D	0.050	0.037	2.34	0.24, −0.23	0.036	0.052	1.59	0.28, −0.31	0.046	0.041	1.96	0.24, −0.21
NEUT_Q	0.049	0.036	2.24	0.24, −0.24	0.035	0.050	1.52	0.28, −0.32	0.045	0.038	1.82	0.21, −0.21
MI_RB_D	0.050	0.038	2.35	0.27, −0.23	0.036	0.052	1.58	0.30, −0.32	0.046	0.040	1.94	0.23, −0.22
MI_RB_Q	0.050	0.036	2.27	0.23, −0.25	0.035	0.050	1.54	0.28, −0.30	0.045	0.038	1.84	0.20, −0.21
RB_D	0.051	0.039	2.42	0.36, −0.26	0.036	0.054	1.65	0.32, −0.30	0.047	0.044	2.09	0.25, −0.20
RB_Q	0.050	0.037	2.33	0.37, −0.28	0.036	0.052	1.59	0.31, −0.31	0.046	0.040	1.93	0.20, −0.20
RB_SH_D	0.050	0.038	2.38	0.28, −0.22	0.036	0.052	1.58	0.30, −0.32	0.046	0.041	1.97	0.24, −0.21
RB_SH_Q	0.050	0.036	2.28	0.24, −0.23	0.036	0.052	1.58	0.28, −0.30	0.045	0.039	1.85	0.21, −0.21
MI_RB_SH_D	0.050	0.037	2.34	0.24, −0.21	0.035	0.051	1.56	0.29, −0.30	0.046	0.040	1.91	0.23, −0.21
MI_RB_SH_Q	0.049	0.035	2.23	0.22, −0.24	0.035	0.050	1.52	0.26, −0.30	0.045	0.037	1.80	0.20, −0.21

Table 3
Results of statistical significance test, λ and σ, for selected pairwise comparisons of models for $DMANH^{+}dCldCA^{-}$.

Model *C*1	Model *C*2	λ	σ	Significant at 0.05%
NEUT_D	NEUT_Q	−0.47	0.02	Yes
MI_RB_D	MI_RB_Q	−0.35	0.02	Yes
RB_D	RB_Q	−0.35	0.02	Yes
RB_SH_D	RB_SH_Q	−0.36	0.02	Yes
MI_RB_SH_D	MI_RB_SH_Q	−0.46	0.02	Yes
NEUT_D	MI_RB_SH_D	−0.17	0.03	Yes
MI_RB_D	MI_RB_SH_D	−0.08	0.02	Yes
RB_D	MI_RB_SH_D	−0.18	0.02	Yes
RB_SH_D	MI_RB_SH_D	−0.24	0.03	Yes
NEUT_Q	MI_RB_SH_Q	−0.07	0.05	No
MI_RB_Q	MI_RB_SH_Q	−0.24	0.03	Yes
RB_Q	MI_RB_SH_Q	−0.30	0.02	Yes
RB_SH_Q	MI_RB_SH_Q	−0.35	0.03	Yes

It is worth emphasizing that the results of this test do not imply which of the models is the correct one. As usual in science, the correct model is unknown. This statistical test estimates the quality of the fitting procedure and is not connected with the chemistry or physics of the phenomena.

3.2. Geometry of hydrogen bonds

For all the compounds, application of mixed refinement (MI_RB_D/Q, MI_RB_SH_D/Q) leads to quite different directions of *X*—H bonds when compared with the standard IAM refinement (RB_D/Q, RB_SH_D/Q; see Fig. 3). The reference *X*—H directions are better reproduced by mixed refinements. For the $DMANH^{+}dCldCA^{-}$ compound, for example, the average difference in the directions of methyl H atoms are 6.4 (21)° for RB_Q refinement and only 2.6 (9)° when the MI_RB_Q procedure is applied. The differences are even more pronounced for H atoms from strong hydrogen bonding. For the N—H direction, the difference is 16.8° for RB_Q refinement and 1.8° for MI_RB_Q, whereas for O—H it equals 4.4° for RB_Q refinement and 1.6° for MI_RB_Q. Much larger differences in the geometry observed for the strongest hydrogen bonds result partially from the fact that the positions of H atoms involved in these interactions were maintained at the values obtained from the IAM or mixed refinement and were not shifted towards standard neutron *X*—H distances.

The different positions of H atoms affect the geometry of hydrogen bonds (see Fig. 4, and Table S1 and Fig. S1 in the supporting materials[3]). The *D*···*A* distances are basically the same for all types of refinements, but the H···*A* distances and the *D*—H···*A* valence angles differ significantly as a function of the method of refinement. The values of the latter differ by up to 6% of the reference parameter for C—H···O hydrogen bonds and up to as much as 32% for strong hydrogen bonds (N···H···N and O···H···O).

At this point our findings differ from the observations reported by Madsen *et al.* (2004). None of their models showed any significant deviation of the direction of the *X*—H bond from the reference data. It is possible that the consequences for strong hydrogen bonds in the above paper were underestimated because of the special positions of the H atoms in the compounds analyzed.

Although one may expect that MI_RB_D/Q and MI_RB_SH_D/Q refinements will give topological parameters closer to the reference values than RB_D/Q or RB_SH_D/Q will, we chose to perform all four types of refinements to explore the degree of difference.

3.3. Dipole *versus* quadrupole truncation

We also decided to check how the level of multipole expansion on H atoms influences their topological properties.

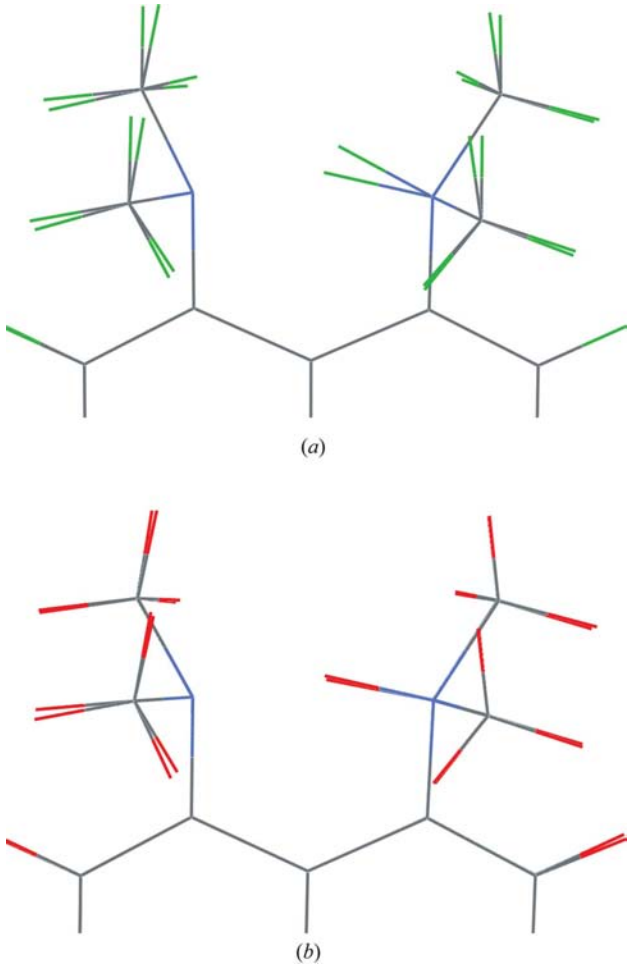

Figure 3
Overlay of the $DMANH^{+}$ cations from $DMANH^{+}dCldCA^{-}$ obtained from NEUT refinement with those from the (*a*) RB_Q and (*b*) MI_RB_Q refinements.

[3] A CIF file containing numerical data for all 30 refinements, and a PDF file containing figures and tables with information regarding all variants of refinements (including dipole and quadrupole truncation levels), geometry of hydrogen bonds, a *PEANUT* illustration (Hummel *et al.*, 1990) of differences between neutron and *SHADE* ADPs, and the numerical values of topological properties for $DMANH^{+}dCldCA^{-}$ are available from the IUCr electronic archives (Reference: CN5018). Services for accessing these data are described at the back of the journal.

Because both truncation levels are widely used in scientific literature, we wanted to make sure that our observations of the consequences of different modeling of H-atom position and motion are general and do not depend on the multipolar truncation level. It appears that the different level of multipolar truncation on H atoms (_D and _Q refinements) generates a diversity in point topological properties (BCPs) of X—H bonds on the same level as different positional or displacement models (see the supporting materials, Fig. S2-5). It is of importance then to use consistently the same multipolar truncation level for the purpose of finding the best way to estimate nuclear parameters of H atoms.

For all the refinement types the same trends are observed. Introduction of quadrupoles on H atoms increases the amount of electron density and decreases the value of the Laplacian at BCPs of X—H bonds This is well illustrated in Fig. 5 for the case of $DMANH^{+}dCldCA^{-}$ and the NEUT_D/Q or MI_RB_SH_D/Q refinement protocols. Integrated atomic properties are less sensitive to the truncation level. Only for H atoms involved in strong hydrogen bonds is the influence significant. The inclusion of quadrupoles increases integrated charges, and decreases the atomic volume and the magnitude of the atomic dipole moment of these atoms. The effect is particularly large for atomic volumes, which become smaller by *ca* 30% after switching on quadrupoles.

Although the agreement between the BCP properties from the NEUT_D/Q and MI_RB_SH_D/Q models is slightly better at the dipole than at the quadrupole level (see Fig. 5, for example), on the basis of the significance of the fit to the experimental data, we choose to discuss the results of the refinement protocols that include quadrupolar expansion on H atoms (_Q).

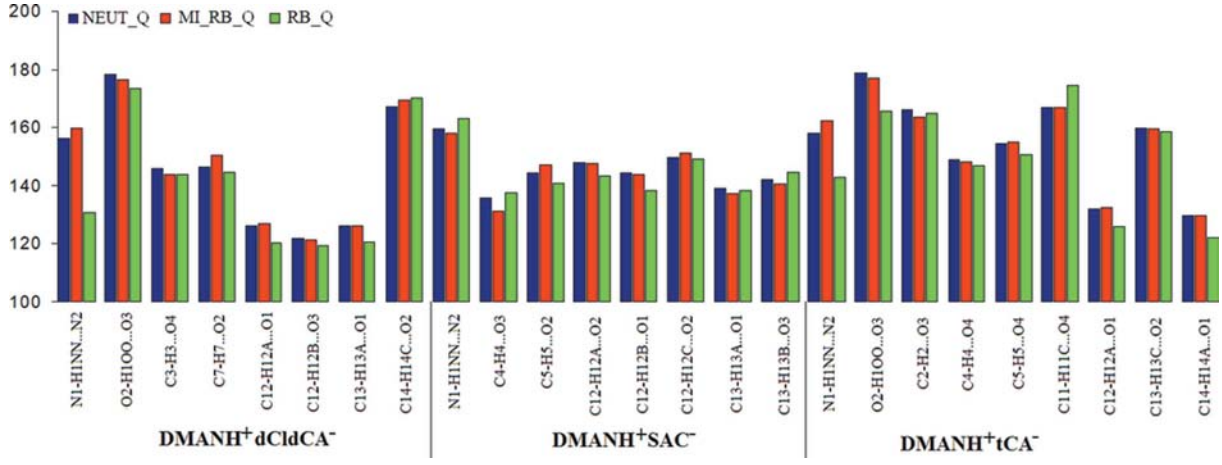

Figure 4
Illustration of the hydrogen-bond structural parameter D—H$\cdots A$ angle (°). Only the three most representative cases of refinement are shown. A typical s.u. for the bond angle is 0.03°.

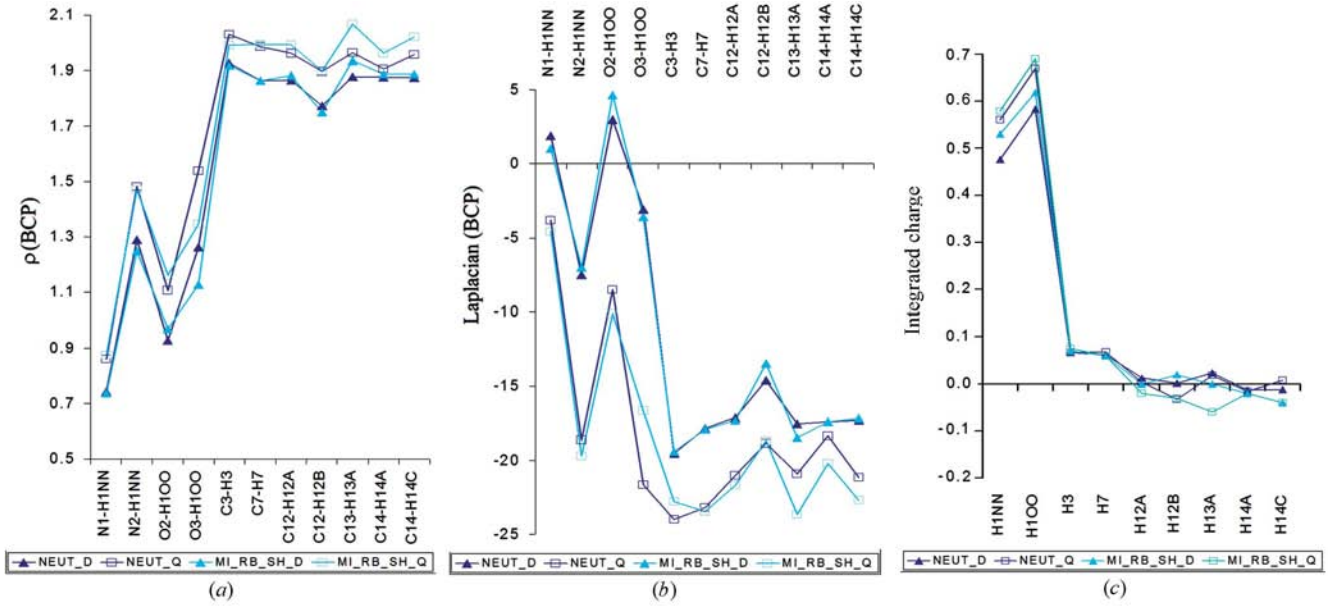

Figure 5
(*a*) Electron density (e Å^{-3}) and (*b*) Laplacian (e Å^{-5}) at BCPs, and (*c*) integrated atomic charge (a.u.) for atoms involved in hydrogen bonds in $DMANH^{+}dCldCA^{-}$. A typical s.u. for the electron density is 0.04 e Å^{-3} and for the Laplacian is 0.14 e Å^{-5}.

3.4. Strong hydrogen bonds

Large discrepancies in the geometrical parameters of strong N···H···N and O···H···O hydrogen bonds affect the BCP properties of these bonds (Fig. 6). The deviations from the reference NEUT_Q values are as large as 1.2 e Å^{-3} and 49 e Å^{-5} for ρ(BCP) and $\nabla^2\rho$(BCP), respectively, that is, more than 100% and as much as 600% of the ρ and $\nabla^2\rho$ values, respectively. The closest values to the reference results are obtained from the MI_RB_SH_Q refinement, with average discrepancies in ρ(BCP) equal to 0.06 Å^{-3} and in $\nabla^2\rho$(BCP) equal to 2.4 e Å^{-5}. The BCP properties obtained from less advanced refinement protocols (RB_Q, MI_RB_Q and RB_SH_Q) deviate significantly more from the reference NEUT_Q data. The average differences in ρ(BCP) and $\nabla^2\rho$(BCP) are 0.30 e Å^{-3} and 7.8 e Å^{-5}, respectively. Apparently, the combination of mixed refinement (the high-angle refinement for non-H atoms and the low-angle refinement for H atoms, and then standardization to the average neutron X—H bond lengths) together with ADPs estimated by the *SHADE* program is the most effective procedure, even when estimated ADPs significantly deviate from the reference ones (see Fig. S6 in the supporting materials).

The integrated atomic properties of H atoms involved in strong hydrogen bonds are significantly influenced by the various treatments of H-atom position and displacement (Fig. 7). The RB_Q refinement leads to significantly underestimated integrated charges, Q, and overestimated integrated volumes, V001 [volume integrated over atomic basins where $\rho(r)$ is greater than or equal to 0.001 a.u.], and atomic dipole moment magnitudes, DM. The results from RB_SH_Q also seem to follow the above trend. The best agreement of all integrated properties with the reference NEUT_Q values are obtained after MI_RB_SH_Q refinement.

3.5. Weak hydrogen bonds

In contrast to the strong hydrogen bonds described above (N···H···N, O···H···O), in weak C—H···O hydrogen bonds

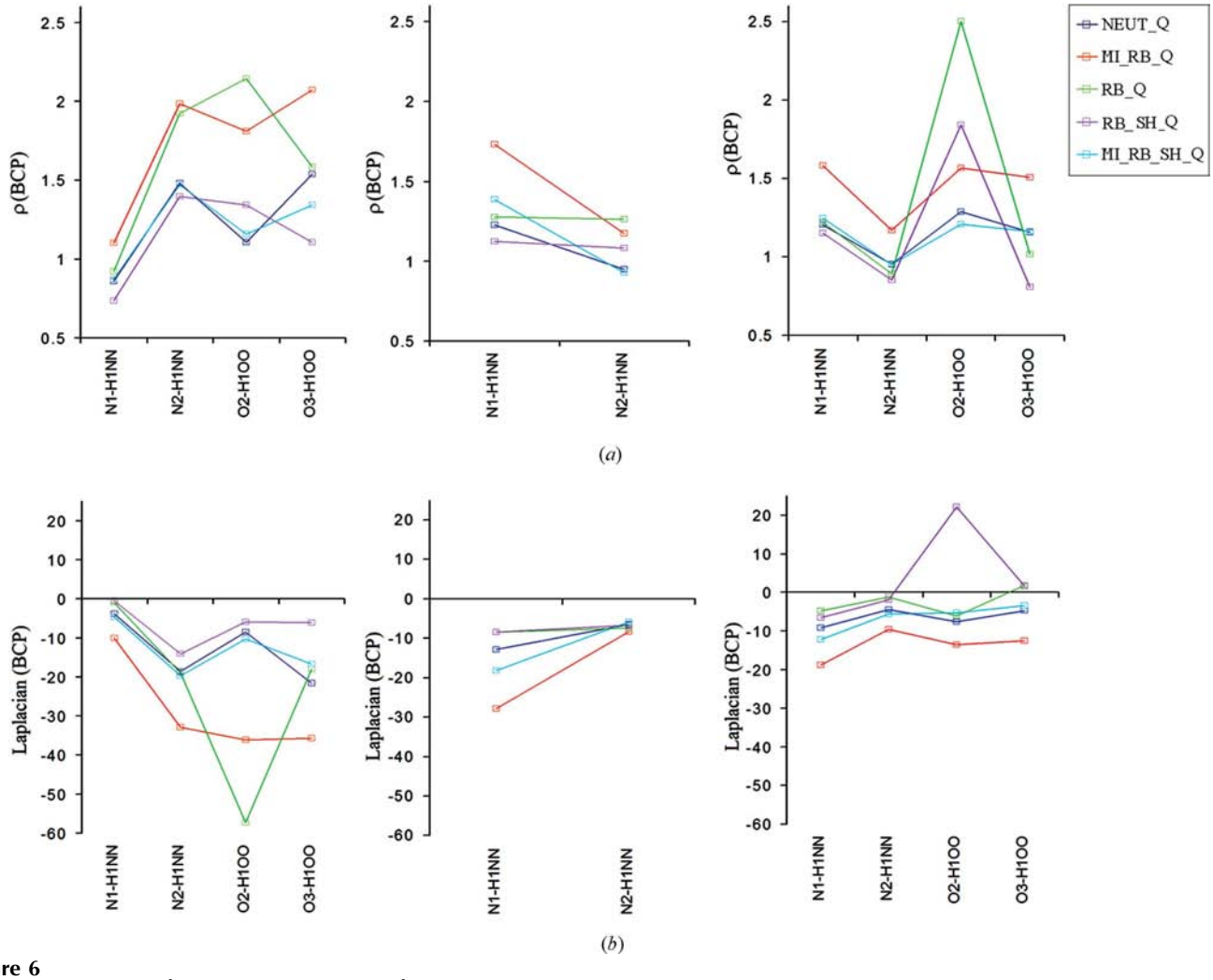

Figure 6
(*a*) Electron density (e Å^{-3}) and (*b*) Laplacian (e Å^{-5}) at BCPs for strong hydrogen bonds (N—H···N and O—H···O) in DMANH$^+$dCldCA$^-$ (left), DMANH$^+$SAC$^-$ (middle) and DMANH$^+$tCA$^-$ (right) calculated by applying different H-atom treatments. A typical s.u. for the electron density is 0.04 e Å^{-3} and for the Laplacian is 0.18 e Å^{-5}.

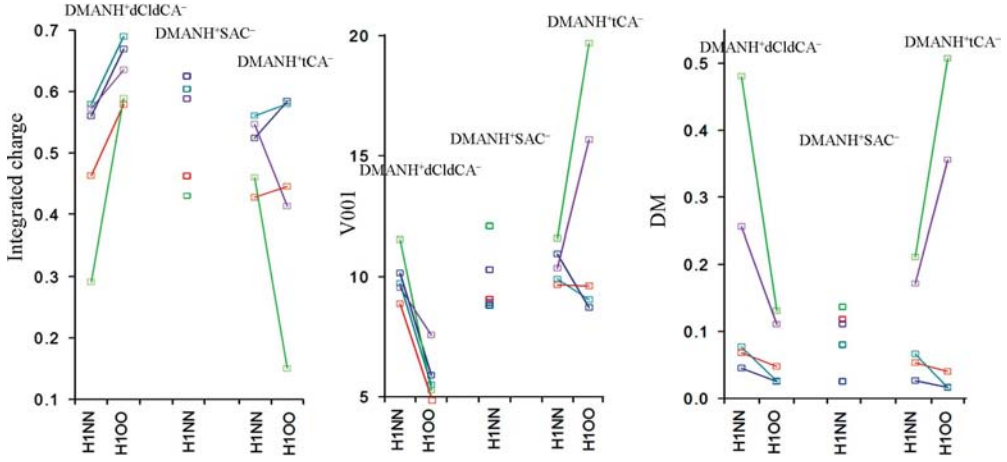

Figure 7
Integrated atomic charge (a.u.; left), integrated atomic volume *V*001 (a.u.; middle) and magnitude of the atomic dipole moment (a.u.; right) for H atoms involved in strong hydrogen bonds in $DMANH^{+}dCldCA^{-}$, $DMANH^{+}SAC^{-}$ and $DMANH^{+}tCA^{-}$ calculated applying different H-atom treatments. For a key to the colors used, see Fig. 6.

there is a clear separation into covalent C—H and non-covalent H···O parts.

For covalent C—H bonds, effects similar to those for strong hydrogen bonds are observed on charge density and Laplacian at the bond critical points (see Fig. 8). Here it is clearly seen that a much better agreement with the reference model was obtained for refinements including ADPs of H atoms (MI_RB_SH_Q and RB_SH_Q) than for those using isotropic (RB_Q and MI_RB_Q) parameters. Evidently, the isotropic displacement parameters used to describe the H-atom thermal motion are not effective enough to provide

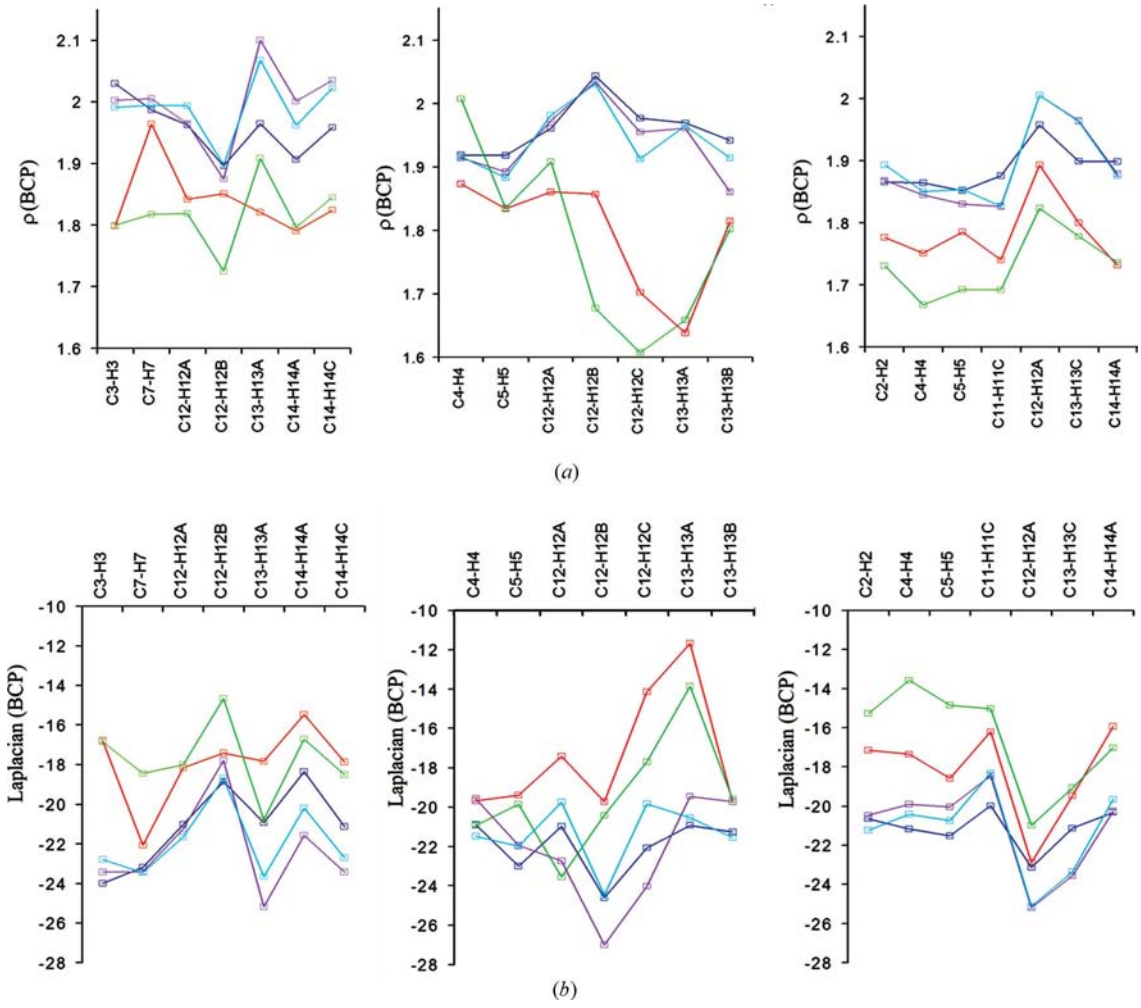

Figure 8
(*a*) Electron density (e Å^{-3}) and (*b*) Laplacian (e Å^{-5}) at BCPs for selected covalent C—H bonds in $DMANH^{+}dCldCA^{-}$ (left), $DMANH^{+}SAC^{-}$ (middle) and $DMANH^{+}tCA^{-}$ (right) calculated by applying different H-atom treatments. A typical s.u. for the electron density is 0.04 e Å^{-3} and for the Laplacian is 0.13 e Å^{-5}. For a key to the colors used, see Fig. 6.

reliable charge densities at BCPs after multipolar refinement. For models with isotropic displacement parameters, the values of ρ(BCP) are systematically lower and the values of $\nabla^2\rho$(BCP) are systematically higher than those of ρ(BCP) and $\nabla^2\rho$(BCP) for the reference NEUT_Q data. Such a relation was described previously (Madsen *et al.*, 2004). The difference in performance between the RB_SH_Q and MI_RB_SH_Q methods for covalent bonds is less pronounced than it was for BCP properties of strong hydrogen bonds. Nevertheless, also in the case of covalent bonds, the MI_RB_SH_Q method gives the best agreement with the reference NEUT values, with the average discrepancies in ρ(BCP) equal to 0.03 e Å^{-3} and in $\nabla^2\rho$(BCP) equal to 1.1 e Å^{-5}.

Comparable (but weaker) trends in ρ(BCP) and $\nabla^2\rho$(BCP) values occur for weak C—H···O hydrogen bonds (see Fig. 9). In this case, the MI_RB_SH method again gives the best agreement, although the precision of the data is lower because the values of the parameters studied are at the limits of the method. Typical residual values of ρ (r.m.s.) are 0.05 e Å^{-3}, whereas the values of the analyzed ρ(BCP) parameters are in the range 0.02–0.11 e Å^{-3}.

There are discrepancies in integrated charge, volume and dipole moment magnitude values obtained from different refinement strategies for H atoms involved in weak hydrogen bonds (see Fig. 10). The best agreement of all integrated properties with the reference NEUT_Q values is obtained after MI_RB_SH_Q refinements. The values of Q, $V001$ and DM obtained from MI_RB_SH refinements differ from the reference results only by about 0.03e, 1 a.u. and 0.04 a.u., respectively. For the RB_Q procedure, the method that is still commonly used in more than 80% of charge-density studies, the values of Q, $V001$ and DM differ the most from the reference values. On average, the discrepancy is as large as 0.16e, 3.4 a.u. and 0.18 a.u. for Q, $V001$ and DM, respectively.

Slightly different trends are observed for DM when compared with the Q and $V001$ results. In the case of Q and $V001$, the methods with ADPs for H atoms give closer results to the reference NEUT data than the methods using isotropic displacement parameters. In the case of DM, all methods without the mixed refinement gave far worse results than the others, probably because of incorrect orientation of the C—H and N—H bonds.

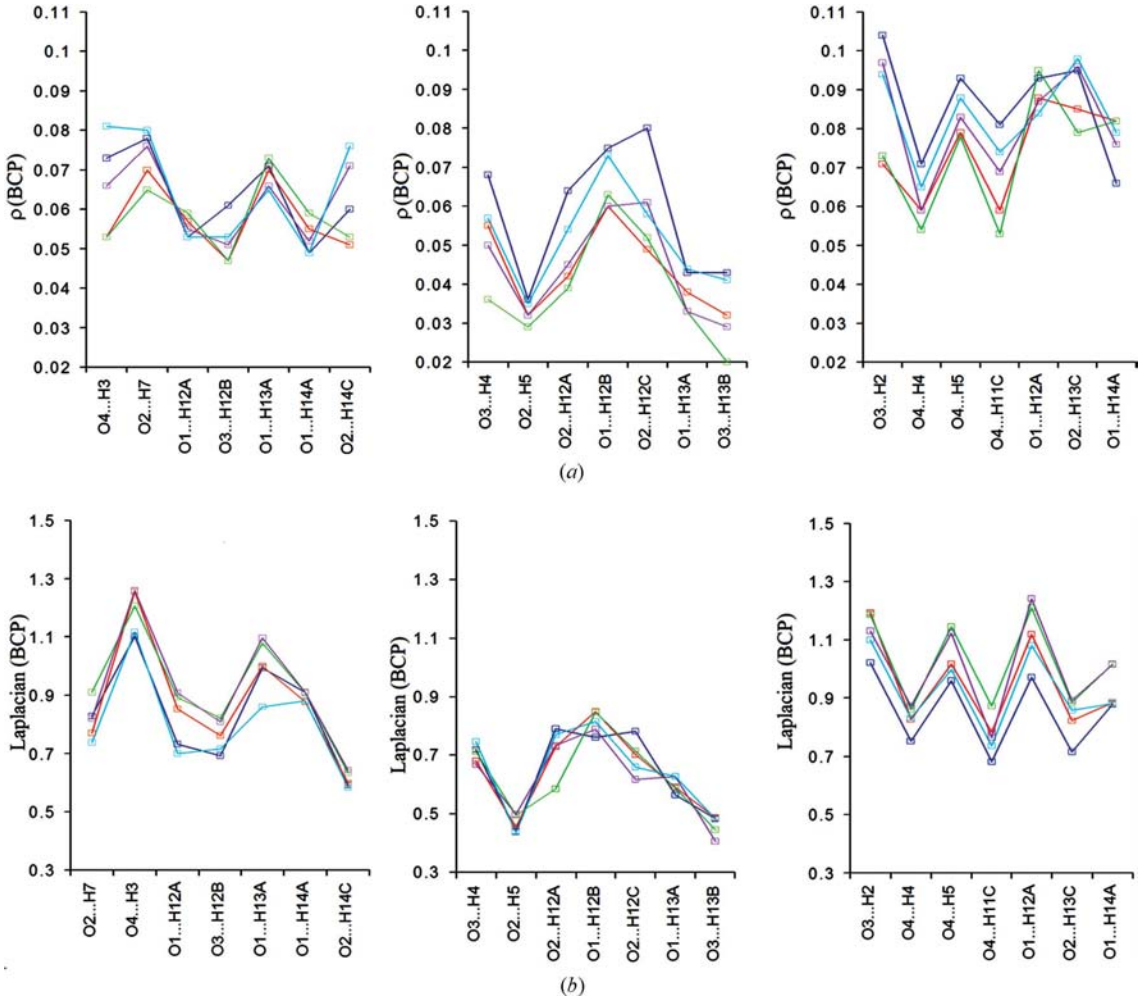

Figure 9
(*a*) Electron density (e Å^{-3}) and (*b*) Laplacian (e Å^{-5}) at BCPs for weak C—H···O hydrogen bonds in DMANH$^+$dCldCA$^-$ (left), DMANH$^+$SAC$^-$ (middle) and DMANH$^+$tCA$^-$ (right) calculated by applying different H-atom treatments. A typical s.u. for the electron density is 0.01 e Å^{-3} and for the Laplacian is 0.01 e Å^{-5}. For a key to the colors used, see Fig. 6.

Somewhat worse agreement of the calculated Q and $V001$ values is obtained for $DMANH^{+}tCA^{-}$, which in our opinion could result from systematic overestimation of the neutron C—H bond lengths in this compound.

3.6. Non-H atoms

It appears that the effect of H-atom treatment on ρ(BCP) and $\nabla^2\rho$(BCP) parameters of the bonds between non-H atoms is negligible (see, for example, Fig. S7 in the supporting

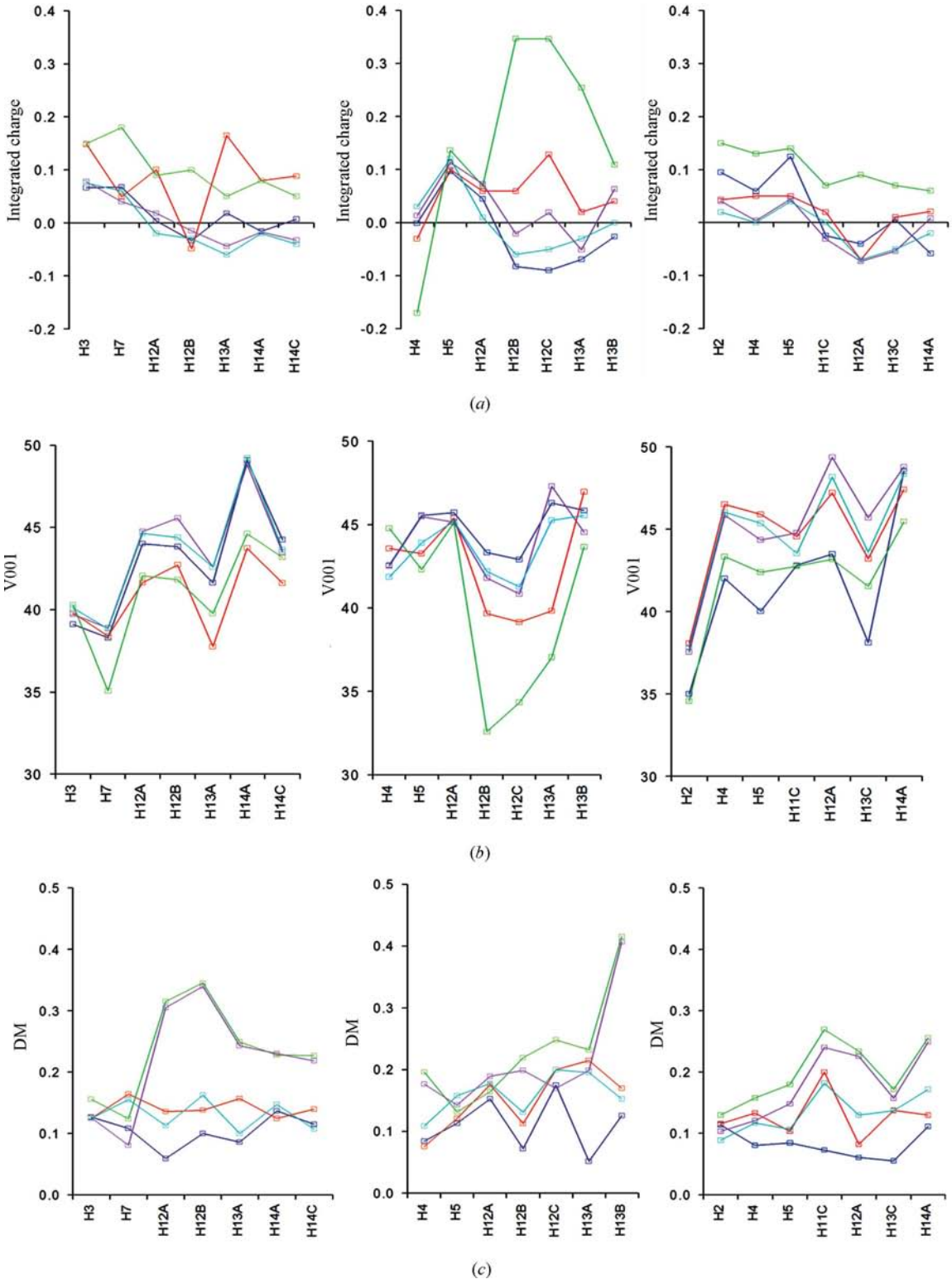

Figure 10
(*a*) Integrated atomic charge (a.u.), (*b*) integrated atomic volume $V001$ (a.u.) and (*c*) magnitude of atomic dipole moment (a.u.) for H atoms involved in weak hydrogen bonds in $DMANH^{+}dCldCA^{-}$ (left), $DMANH^{+}SAC^{-}$ (middle) and $DMANH^{+}tCA^{-}$ (right) calculated by applying different H-atom treatments. For a key to the colors used, see Fig. 6.

materials). However, the integrated properties of the non-H atoms to which at least one H atom is attached depend on the refinement protocol (see, for example, Fig. 11, and Fig. S8 in the supporting materials). The greater the number of covalently bonded H atoms, the larger are the discrepancies between integrated values obtained from any given refinement protocol and the referential value.

In the case of $DMANH^{+}dCldCA^{-}$, the largest differences between the values of Q, $V001$ and DM obtained after the NEUT_D, MI_RB_SH_D and RB_D refinements are observed for methyl C atoms (C11, C12, C13 and C14), with smaller – but still important – differences observed for aromatic C atoms and negligible differences for C atoms that are not bonded to H atoms (*i.e.* C20 and C21). The values of integrated charge obtained after the RB_D procedure on non-H atoms are systematically smaller than those obtained from NEUT_D. This agrees well with the behavior of the integrated charge values of H atoms, which are systematically higher for the RB_D method. An opposite situation is seen for the integrated volume: its values are overestimated for non-H atoms and underestimated for H atoms.

The values of Q, $V001$ and DM obtained after the MI_RB_SH_D procedure are in better agreement with the reference NEUT_D data than those from RB_D.

4. Conclusions

According to our study, to obtain the best topological parameters in the case of a lack of neutron data, a mixed refinement (high-order refinement of heavy atoms, low-angle refinement of H atoms and elongation of the X—H distance to the average neutron bond lengths) supplemented by an estimation of anisotropic thermal motion of H atoms should be applied.

The proposed refinement strategy leads to a good agreement of topological parameters with those from the reference data, even in the case of strong hydrogen bonding (N···H···N and O···H···O). This may result from the improvement of geometrical parameters obtained from the mixed refinement. In the case of weak hydrogen bonds (C—H···O), quite a good agreement of electron density, the Laplacian at bond critical points, and integrated charges and volumes with the reference values was obtained not only after the MI_RB_SH methods but also after the RB_SH procedure. However, the differences in geometry and in dipole moment magnitudes also favor the MI_RB_SH refinement. Although we did not test our strategy for moderately strong hydrogen bonds (X—H···Y), one may assume that it should work as well for them as for the strong and weak hydrogen bonds discussed in this work.

Apparently, the standardization of X—H distance to the average neutron data without any additional improvement of ADPs and X—H directions is not sufficient to obtain correct topological parameters for the atoms.

It appears that the magnitude of the differences in the values for the point and integrated topological properties as a function of the method of H-atom treatment is unexpectedly large. Therefore, in our opinion, topological and integrated properties calculated for H and non-H atoms obtained by using different models of H atoms should not be compared.

KW thanks the Ministry of Science and Higher Education for financial support (grant No. 1 T09A 116 30. PMD acknowledges support from Iceland, Liechtenstein and Norway for a grant received through the EEA Financial Mechanism and the HOMING Programme of the Foundation for Polish Science (Edition 2007), and from grant 501/68-BW-175601. AAH and KW thank the Foundation for Polish Science for support within the 'MASTER (Mistrz)' programme.

References

Allen, F. H., Kennard, O., Watson, D. G., Brammer, L., Orpen, A. G. & Taylor, R. (1987). *J. Chem. Soc. Perkin Trans. 2*, pp. S1–19.

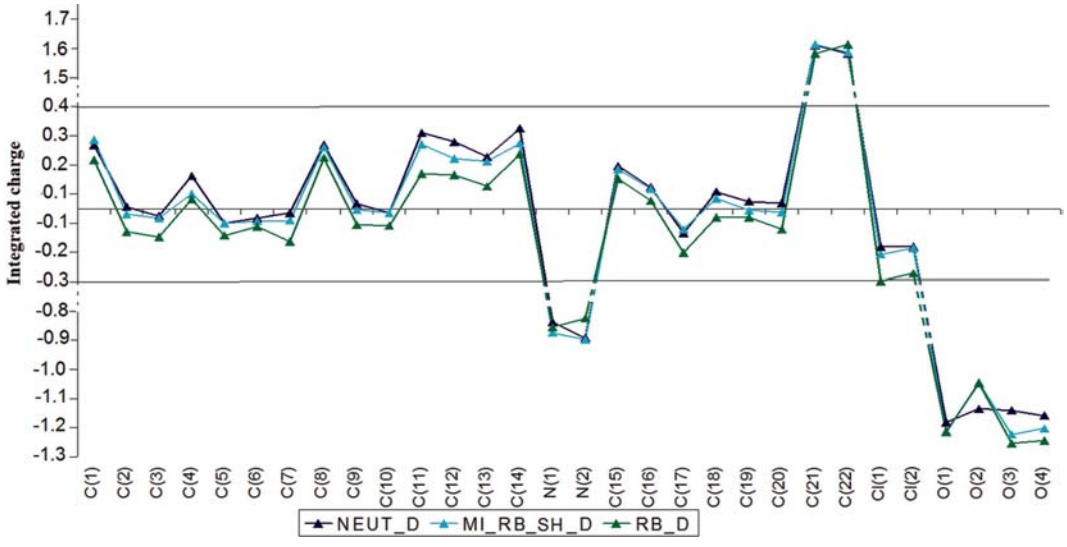

Figure 11
Integrated atomic charge (a.u.) calculated for non-H atoms for $DMANH^{+}dCldCA^{-}$ by use of three different H-atom models.

Chen, L. & Craven, B. M. (1995). *Acta Cryst.* B**51**, 1081–1097.
Destro, R. & Merati, F. (1995). *Acta Cryst.* B**51**, 559–570.
Dominiak, P. M., Makal, A., Mallinson, P. R., Trzcinska, K., Eilmes, J., Grech, E., Chruszcz, M., Minor, W. & Woźniak, K. (2006). *Chem. Eur. J.* **12**, 1941–1949.
Eisenstein, M. & Hirshfeld, F. L. (1983). *Acta Cryst.* B**39**, 61–75.
Espinosa, E., Lecomte, C. & Molins, E. (1999). *J. Chem. Phys.* **300**, 745–748.
Espinosa, E., Molins, E. & Lecomte, C. (1998). *J. Chem. Phys.* **285**, 170–173.
Espinosa, E., Souhassou, M., Lachekar, H. & Lecomte, C. (1999). *Acta Cryst.* B**55**, 563–572.
Flaig, R., Koritsanszky, T., Zobel, D. & Luger, P. (1998). *J. Am. Chem. Soc.* **120**, 2227–2238.
Harel, M. & Hirshfeld, F. L. (1975). *Acta Cryst.* B**31**, 162–172.
Hirshfeld, F. L. (1976). *Acta Cryst.* A**32**, 239–244.
Hirshfeld, F. L. & Hope, H. (1980). *Acta Cryst.* B**36**, 406–415.
Hummel, W., Hauser, J. & Bürgi, H.-B. (1990). *J. Mol. Graphics*, **8**, 214–220.
Koch, U. & Popelier, P. L. (1995). *J. Phys. Chem.* **99**, 9747–9754.
Kocher, N., Selinka, C., Leusser, D., Kost, D., Kalikhman, I. & Stalke, D. (2004). *Z. Anorg. Allg. Chem.* **630**, 1777–1793.
Koritsanszky, T., Howard, S., Su, Z., Mallinson, P. R., Richter, T. & Hansen, N. K. (1997). *XD*. Version 4.09. Free University of Berlin, Germany.
Koritsanszky, T. S. & Coppens, P. (2001). *Chem. Rev.* **101**, 1583–1627.
Madsen, A. Ø. (2006). *J. Appl. Cryst.* **39**, 757–758.
Madsen, A. Ø., Sørensen, H. O., Flensburg, C., Stewart, R. F. & Larsen, S. (2004). *Acta Cryst.* A**60**, 550–561.
Mallinson, P. R., Smith, G. T., Wilson, C. C., Grech, E. & Wozniak, K. (2003). *J. Am. Chem. Soc.* **125**, 4259–4270.
Munshi, P., Madsen, A. Ø., Spackman, M. A., Larsen, S. & Destro, R. (2008). *Acta Cryst.* A**64**, 465–475.
Prince, E. & Spiegelman, C. H. (1995). *International Tables for Crystallography*, Vol. C., edited by A. J. C. Wilson, pp. 618–624. Dordrecht: Kluwer Academic Publishers.
Roversi, P., Barzaghi, M., Merati, F. & Destro, R. (1996). *Can. J. Chem.* **74**, 1145–1161.
Roversi, P. & Destro, M. (2004). *Chem. Phys. Lett.* **386**, 472–478.
Sheldrick, G. M. (2008). *Acta Cryst.* A**64**, 112–122.
Spackman, M. A. (1992). *Chem. Rev.* pp. 1769–1797.
Spackman, M. A. (1999). *Chem. Phys. Lett.* **301**, 425–429.
Spackman, M. A. & Byrom, P. G. (1996). *Acta Cryst.* B**52**, 1023–1035.
Spackman, M. A., Byrom, P. G., Alfredsson, M. & Hermansson, K. (1999). *Acta Cryst.* A**55**, 30–47.
Spackman, M. A., Munshi, P. & Dittrich, B. (2007). *Chem. Phys. Chem.* **8**, 2051–2063.
Staab, H. A. & Saupe, T. (1988). *Angew. Chem. Int. Ed. Engl.* **27**, 865–879.
Stewart, R. F. (1991). *The Application of Charge Density Research to Chemistry and Drug Design*, edited by G. A. Jeffrey & J. F. Piniella, pp. 63–101. New York: Plenum Press.
Volkov, A., Abramov, Y. A. & Coppens, P. (2001). *Acta Cryst.* A**57**, 272–282.
Volkov, A., Gatti, C., Abramov, Y. & Coppens, P. (2000). *Acta Cryst.* A**56**, 252–258.
Wolstenholme, D., Aquino, M. A. S., Cameron, T. S., Ferrara, J. D. & Robertson, K. N. (2006). *Can. J. Chem.* **84**, 804–811.
Woźniak, K., Mallinson, P. R., Smith, G. T., Wilson, C. C. & Grech, E. (2003). *J. Phys. Org. Chem.* **16**, 764–771.